第 49 卷第 1 期
七月 2024

Vol. 49 No. 1
2024

Diqiu Kexue - Zhongguo Dizhi Daxue Xuebao/Earth Science
Journal of China University of Geosciences
https://dqkx-periodicals.com

https://doi.org/10.3799/dqkx.2024.5632

Determining the causes of longitudinal cracks on the slopes of concrete canals

Masharif Bakiev[a], Bakhadir Kulumbetov[b], Khojiakbar Khasanov[c]

[a] "Tashkent Institute of Irrigation and Agricultural Mechanization Engineers" National Research University, 10000 Tashkent, Uzbekistan, bakiev1947@rambler.ru
[b] "Tashkent Institute of Irrigation and Agricultural Mechanization Engineers" National Research University, 10000 Tashkent, Uzbekistan, bp_kulumbetov@mail.ru
[c] "Tashkent Institute of Irrigation and Agricultural Mechanization Engineers" National Research University, 10000 Tashkent, Uzbekistan, kh.khasanov@mail.ru

Received: 13 March 2024

Accepted: 16 April 2024

Published: 24 April 2024

Abstract: In the Republic of Karakalpakstan in Uzbekistan, characterized by a sharply continental climate and precipitation of less than 150 mm per year, saline soils and groundwater with high salt concentrations are widely distributed. The situation is exacerbated by the drying up of the Aral Sea and the appearance of salt aerosols in the region. The Bustan Canal is in this area and is intended for irrigating 100,000 hectares of farmland. The reconstruction of the canal allows for the abandonment of mechanical irrigation and the transition of the system to gravity irrigation. After the canal was put into operation, longitudinal cracks appeared at three stations: 47+20, 202+80, and 218+00. To identify the causes, concealed work was carried out at these locations where cracks appeared. Laboratory analysis of water and soil was conducted to examine the concrete strength, soil particle size distribution, and free swell index. This article presents the results of water analysis for concrete and its maintenance, as well as chemical analysis of the soil. All analyses were performed in licensed laboratories following the relevant national standards. Water for moistening the soil to optimal moisture during embankment construction, for concrete, and for concrete maintenance was sourced from two wells drilled at PK 183+20 and PK 218+45. The analysis showed that the pH of the water was between 4 and 12.5, with a value of 8.2. The sulfate ions (SO4) were 845.54 mg/L, below the limit of 2700 mg/L; chloride ions were 222.7 mg/L, below the limit of 4500 mg/L; suspended particles were 800 mg/L, exceeding the norm of 300 mg/L. The total content of sodium ions (Na+) and potassium ions (K+) was 319.47 mg/L, below the norm of 1500 mg/L. The water from the wells did not contain films of petroleum products, oils, fats, or coloring impurities. Overall, the water was suitable for concrete and concrete maintenance. Further compression strength tests on the concrete showed that the design strength of V 15 (M200) was achieved. The chemical analysis of the soil was conducted using the water and salt-acid extraction method. The sum of the percentage contents of the main ions ranged from 0.159% to 0.289%, indicating a low degree of overall salinity. The content of sulfate ions reached 37.5 eq.%, and sodium and potassium cations reached 41.951 eq.%. The gypsum content was 1.185%, which is below the norm of 5%. The soil was not gypsumized and was sulfide-stable. The soil pH was within the normal range, at pH = 7.4 ± 7.6.

Keywords: *Bustan Canal, longitudinal cracks, concrete strength, water analysis, pH, subsidence, optimal humidity, maximum density.*

1. Introduction

The formation of cracks in concrete canals violates the integrity of the fastening, as a result, reduces the reliability of filtration and static stability.

Research (Hu, Li, & Wang, 2023) studied the south-north water transmission canal in China. Using the LSSVM algorithm, the problem of predicting the displacement of slopes of canals with a high groundwater level was implemented. In research (He, Dong, Ren, & Wu, 2021), the destruction of concrete cannel fastenings due to frost heaving is considered. It has been established that those dangerous areas are located at the beginning and end of transition sections. The canal lining under conditions of uneven frost heaving was analyzed. In research (Zhu, Huang, Zhang, Guo, & Chen, 2022), laboratory and centrifugal model studies of the destruction of canal slopes under conditions of periodic moistening and drying were carried out. Failure was detected at the canal water level with further spalling below this level. Research (Liu et al., 2021) notes that in cold weather conditions, damage to canal slopes often occurs as a result of frost heave. Three types of slope protection structures were studied: insulation concrete slabs, concrete lining and pebbles. A hinged connection of slabs to protect against frost heaving is proposed. In (Wang, Zhang, Li, & Liu, 2023), a mechanical model of trapezoidal canal lined with two-layer geomembranes was developed. During the period of freezing in traditional concrete fastenings, they are maximum, and during thawing, the opposite is true. Research (Yao et al., 2012) presents studies of filtration from canals with a lining and a multilayer base. The HYDRUS-2D numerical model was used and compared with the results of field studies. Clay liners showed the more filtration, followed by compacted layers in second place, followed by pebbles and concrete liners. (Taran & Mahtabi, 2020) investigated concrete canals on the influence of uplift pressure and hydraulic gradient at different groundwater levels. The simulation was carried out using the SEEP/W model in the presence of drainage holes on the bottom and slopes of the canal.

Article (H. Rahimi & Barootkoob, 2002) presents the results of field and laboratory studies for the causes of cracking in a concrete canal in the Iranian province of Khuzistan. The research included chemical-mechanical analysis of borrow area soil and canal embankment. The soils had low and medium plasticity; the content of soluble substances was less than 1%. The main cause of cracking was identified as low water content during compaction and low moisture content during canal lining, which resulted in high free swelling. Testing was performed using ASTM and JSSMFE methods. Article (Hassan Rahimi & Abbasi, 2008) the results of a study for the causes of destruction of the Save irrigation concrete lining canal are presented. Field studies were carried out along the axis of the embankment every 500 m and sampling every 50 cm. The main soils are sandy, that is, non-dispersed, but some samples are classified as chemically highly dispersed. The main causes of damage were determined as design parameters, quality of construction and geotechnical properties of the soil. In article (Hassan Rahimi, Abbasi, & Shantia, 2011) examines the Mogan irrigation and drainage network in Iran. Geotechnical studies of an embankment made of fine sand and loess were carried out. Under the influence of filtration, fine sand was washed out from under the concrete, which led to the destruction of the lining; It was recommended to install a geomembrane under the concrete cladding. The Bustan project in this sense is made with a geomembrane. In research (Ahmadi, Rahimi, & Abdollahi, 2009), using finite element models, the influence of the elastic modulus and Poisson's ratio on the magnitude of bending moments and deformations was studied. It is recommended to install the longitudinal seam at 1/3 of the depth of the canals. The research (Belendir, Ivashintsov, & Stefanyshyn, 2004) discusses general methods for assessing the reliability of infiltration in soil structures. In (Iskandar, Dinar Dwi Anugerah, & Putri Kusuma, 2021), the issues of reconstruction of an

irrigation canal in Indonesia with different types of linings are considered: brick, prefabricated slabs and concrete. It is noted that the best option is concrete lining. Studies (Kosichenko, 2006; Kosichenko, Bae, & Ishchenko, 2014; Kosichenko & Baev, 2020) consider the issues of filtration losses from ground canals and with support, methods for their calculation, modern control methods and operational reliability of structures. Our article (Bakhodir, Masharif, & Quvochbek, 2023) presents the results of field studies of the water tightness of concrete lining on the Bustan Canal. In (Kulumbetov B.P., Bakiev M.R., 2023), the characteristics of soils during the construction of the Bustan canal embankment and the technology of its construction are described when groundwater higher than the canal bed. In (Lunyov A.A., 2019), the use of ash and slag mixtures in the construction of highway embankments was investigated and justified. The physical properties, particle size distribution, humidity and density of ash and slag have been established. GOSTs (GOST 22733-2002, 2002; GOST 25100-2020, 2020; GOST 28514-90, 1990) provide for the classification of soils and methods for laboratory studies of optimal moisture and maximum density.

2. Method

Using a cutting device, we cut off the concrete lining on three picket fences where cracks appeared. The condition of the geomembrane and geotextile was examined visually. The strength of concrete during the construction period was assessed based on laboratory tests of three cubes, the average values were determined and compared with the designed values. Hydraulic presses PSU-125 and ETK-111, scales VNTs-10, calipers ShchTs-250 and ShchTs-11 were used. Soil samples were taken at each picket PK 202+80 and PK218+00, as well as two samples at picket 47+20. The studies were carried out in the OLI laboratory of RCIIL LLC in order to determine the physical, mechanical and chemical properties, as well as subsidence and free swelling of soils. The particle size distribution was previously determined by the aerometric method in accordance with the method described in GOST 12536-2014. Optimal humidity and maximum dry density were determined by the method in accordance with the standards RST.Uz7896-97 and GOST 22733-2002 and GOST 25100-95.

Figure 1. *Sampling and laboratory research*

3. Research results

The particle size distribution was previously determined by the aerometric method in accordance with the procedure described in GOST 12536-2014. In table 1 and in Figure 1 presents the results of determining the particle size distribution of soils in the western part of the canal.

As can be seen from Table 1, the material in its particle size distribution and plasticity number corresponds to GOST 25100-95. (table B.11): PK 202+80 - sandy loam; PK 218+00 – sandy loam; PK47+20(1) - at the border of sandy loam and loam; PK47+20(2) - sandy loam.

Table 1. *Results of laboratory determinations of the physical properties of object soils*

№	Location	Content particles in %								Plasticity		
		1.0-0.5mm	0.5-0.25mm	0.25-0.1mm	0.1-0.05mm	0.05-0.01mm	0.01-0.005mm	0,005-0.002mm	< 0.002mm	W_L	Wp	Jp
1	ПК 202+80		1.2	2.3	35.0	48.2	13.3			22.8	18.8	4.0
		100.0	100.0	98.8	96.5	61.5	13.3	0.0				

2	ПК 218+00		1.6	2.9	35.2	47.6	11.5	1.2		22.6	18.5	4.1
		100.0	100.0	98.4	95.5	60.3	12.7	1.2				
3	ПК 47+20 (1)		1.5	3.5	21.6	45.9	25.6	1.9		31.7	23.7	8.0
		100.0	100.0	98.5	95.0	73.4	27.5	1.9				
4	ПК 47+20 (2)	2.4	6.2	13.4	42.1	30.5	5.4			19.5	17.3	2.3
		100.0	97.6	91.4	78.0	35.9	5.4	0.0				

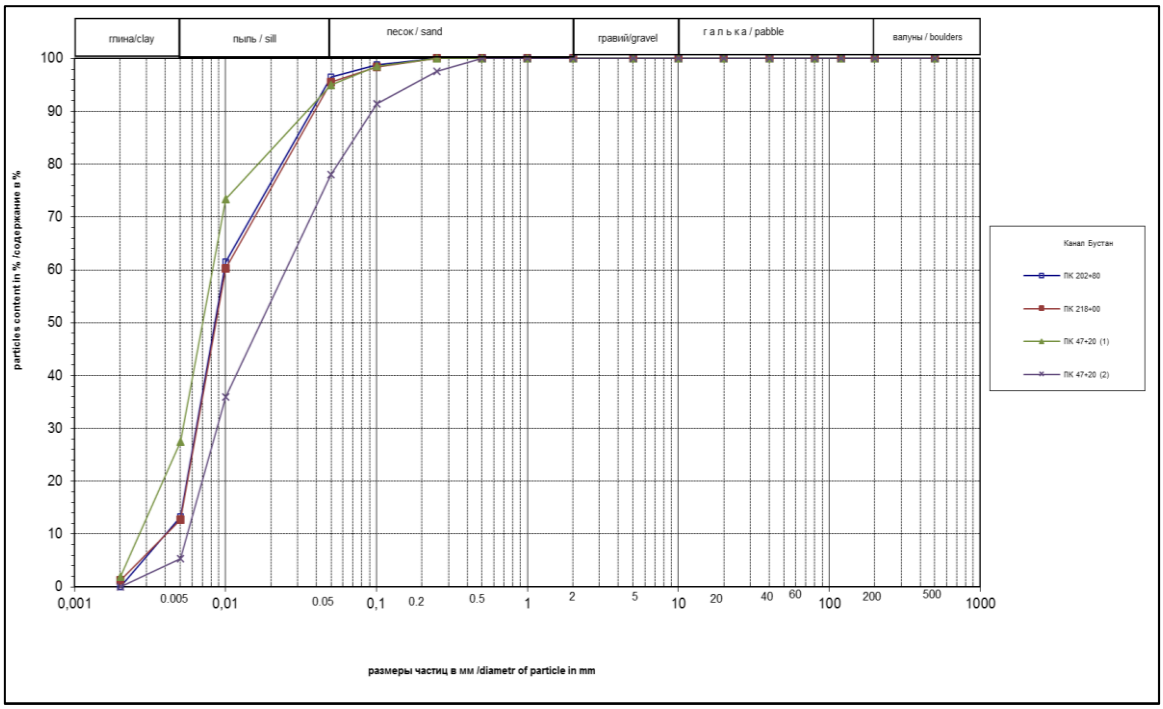

Figure 2. *Particle size distribution of the soil.*

Table 2. *Table of indicators of physical and mechanical properties of soils*

Sampling location		**ПК 202+80**	**ПК 218+00**	**ПК 47+20 (1)**	**ПК 47+20 (2)**
Density of Particle size. g/см^3		2.66	2.66	2.69	2.66
Density of soil. g/см^3		2.12	2.11	1.99	1.81
Dry density. g/см^3		1.86	1.85	1.78	1.6
Porosity. %		30.1	30.4	33.9	39.8
Coefficient Porosity.		0.43	0.44	0.51	0.66
Natural humidity. w		14	14	12	13
Humidity level. Sr		0.87	0.85	0.63	0.52
Plasticity %	w_L	22.8	22.61	31.69	19.52
	w_P	18.77	18.54	23.73	17.25
	I_P	4	4.1	8	2.3
Single-plane cut	ϕ deg.	28.22	30.98	23.48	27.22
	C кPa	21.3	25.2	31	14

Compression modulus. E/E_w. MPa	E MPa	15.56	25.89	2.74	2.74
	Ew MPa	13.53	19.16	2.34	1.97
Relative subsidence strain	P =0.1 MPa	0.001	0.001	0.014	0.006
	P =0.2 MPa	0.001	0.002	0.017	0.007
	P =0.3 MPa	0.001	0.001	0.019	0.009

As can be seen from Table 2. for three samples the relative subsidence strain is less than 0.01. i.e. the soil is non-subsidence. and for the first sample with PC 47+20 it changes from 0.014 to 0.019. i.e. subsidence soil. This may cause cracks at this location.

Regulatory documents oblige. before the construction of an earthen canal. to carry out trail compaction and laboratory studies on the compaction of soils intended for the construction of a embankment.

Usually. before experimental rolling on embankments. preliminary laboratory compaction is preceded. which makes it possible to establish the dependence of soil moisture and density during various compaction work.

Laboratory compaction. in contrast to field conditions. is carried out not by rolling. but by compacting the soil in accordance with the standard rules available in this regard. Despite the conventionality of the standard compaction method. varying the value of the specific compaction work makes it possible to establish good connections between the amount of work of the standard compaction and the type and weight of the soil compaction mechanism. To do this. it is necessary to compact the soil using various specific compaction works.

Standards. depending on the purpose. height and class of the structure. provide for the use of various compaction work. with the main difference being the weight. the height of the load. as well as the number of layers of compacted soil in the container. The work spent on soil compaction in laboratory conditions is represented by the formula:

$$A = \frac{\rho_{тр} \cdot H \cdot n \cdot N}{V}. \quad (1)$$

where: $\rho_{тр}$- tamper mass. kg; H - cargo release height. cm; n is the number of hits on the layer; N – number of layers; V – container volume.

Based on the results of compaction. graphs of the dependence of density on humidity are constructed for various specific works spent on compaction.

The method for determining the maximum density is used in accordance with RST.Uz 7896-97 and GOST 22733-2002. which regulate the standards given in table. 3. and involves testing in a device developed at the SOYUZDORNII Institute for standard soil compaction.

Table 3. *Determining Maximum Density*

№ standards	**Kettlebell weight**	**Number of layers (pcs.)**	**Hight of load (см)**	**Number of hits (pcs.)**	**Specific work. (гсм/см^3)**	**Weight of rolls (ton.)**
1	2.5	3	30	25	A_1-5600	Up to 20

2	2.5	5	30	25	A_2-9370	20-40
3	4.5	3	46	25	A_3-15500	40-80
4	4.5	5	46	25	A_4-25900	>80

Standard No. 1 is mandatory to obtain soil characteristics with minimal compaction work. Standard No. 3 regulates laboratory compaction of soils intended for critical structures. For intermediate specific compaction work. a method with an increased number of compaction layers is selected (standard No. 2. then we will have the following standards: 1. 2 and 3 or 1. 3 and 4).

Based on the values of density and humidity of compacted samples obtained as a result of tests. the density of dry soil is determined with an error of up to 0.01 g/cm3 using the formula:

$$\rho_{ck} = \frac{\rho_w}{1+W}. \quad (2)$$

Where ρ_{ck} is the density of dry soil; ρ_w- density of wet soil. W – humidity in fractions of a unit.

A graph was made of the dependence of density on soil moisture. plotting the moisture content of compacted samples on the abscissa axis. and soil density on the ordinate axis. Find the maximum of the obtained dependence and the corresponding values of maximum density and optimal humidity. The test results are presented in table 4. in fig. 3. 4. 5. 6.

Table 4. *Results of laboratory soil testing*

Standards	**W_{opt}. %**	**$\rho_{мак}$. g/cm³**
A1	13÷15	1.85
A1	13÷15	1.86
A1	13÷15	1.78
A1	13÷15	1.60

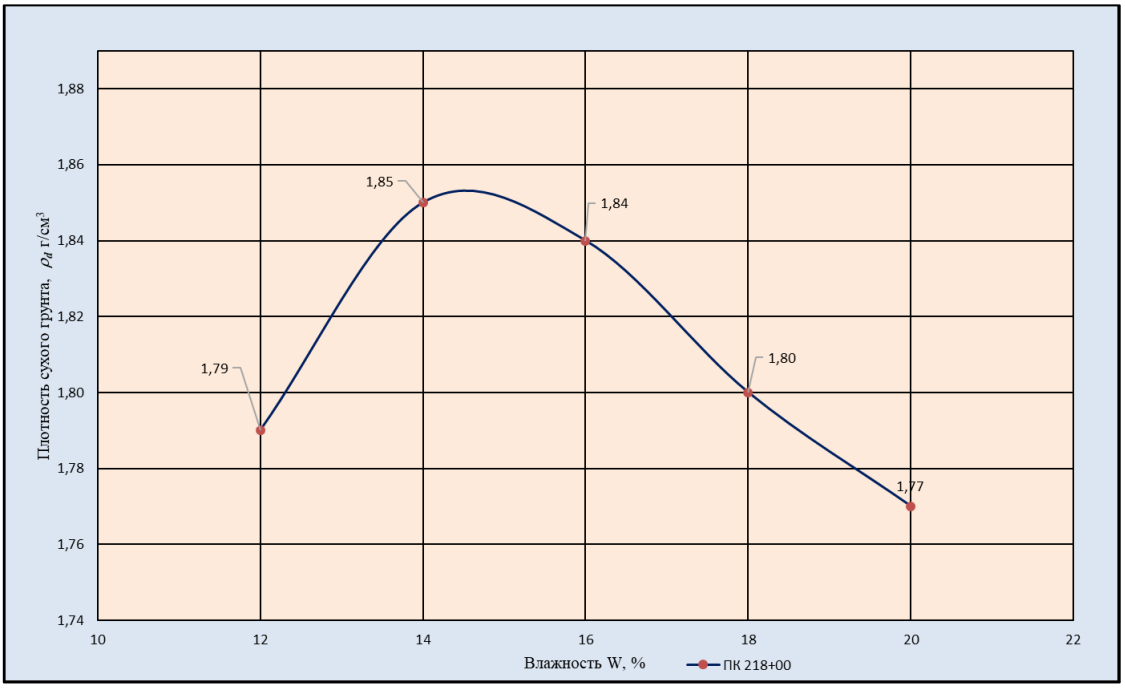

Figure 3. *Graph of the dependence of the maximum soil density on the optimal humidity. PK218+00. Standard A1.*

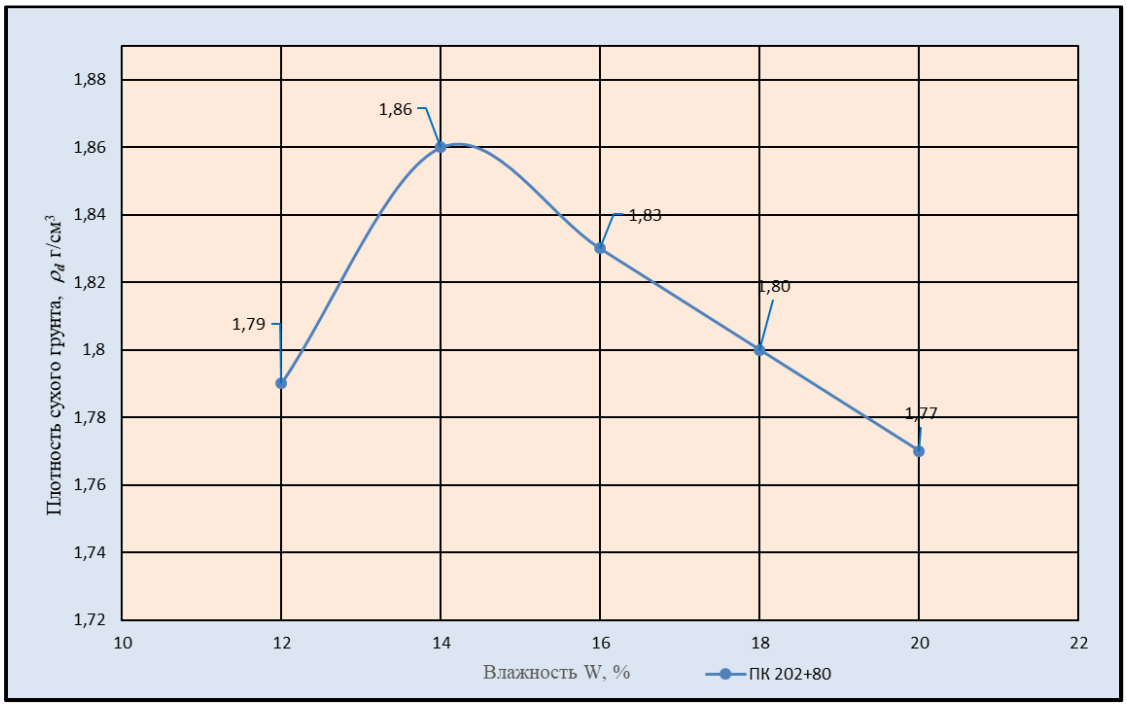

Figure 4. *Graph of the dependence of the maximum soil density on the optimal humidity. PK202+80. Standard A1.*

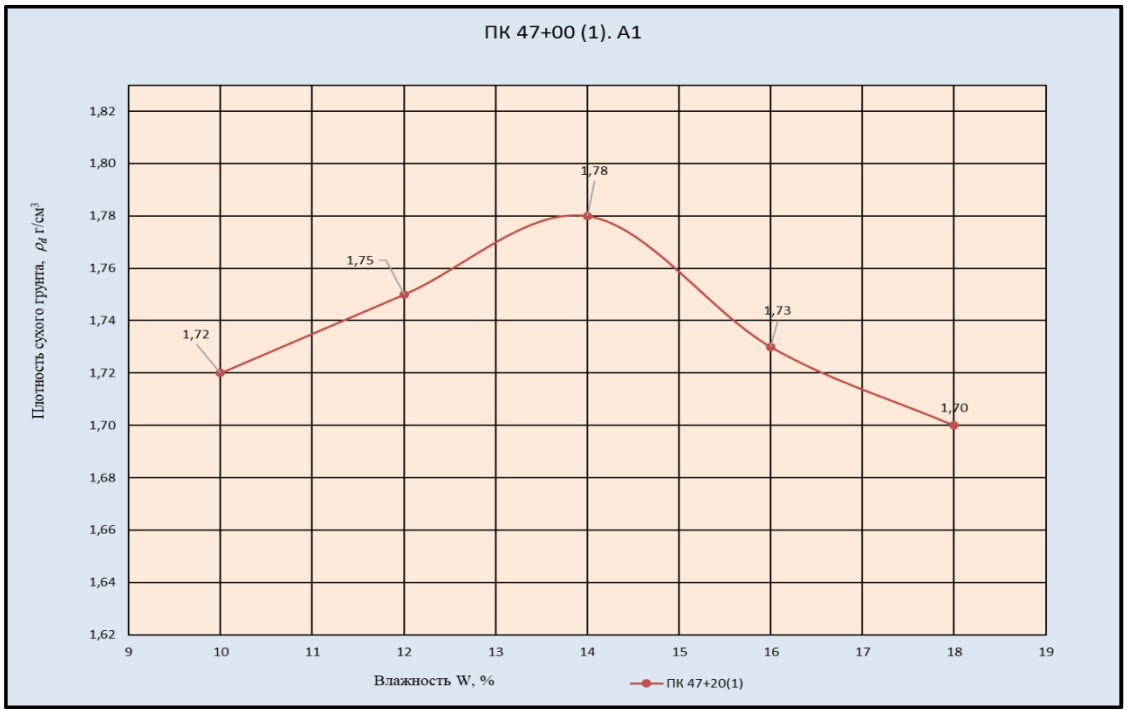

Figure 5. *Graph of the dependence of the maximum soil density on the optimal humidity. PK47+20(1). Standard A1.*

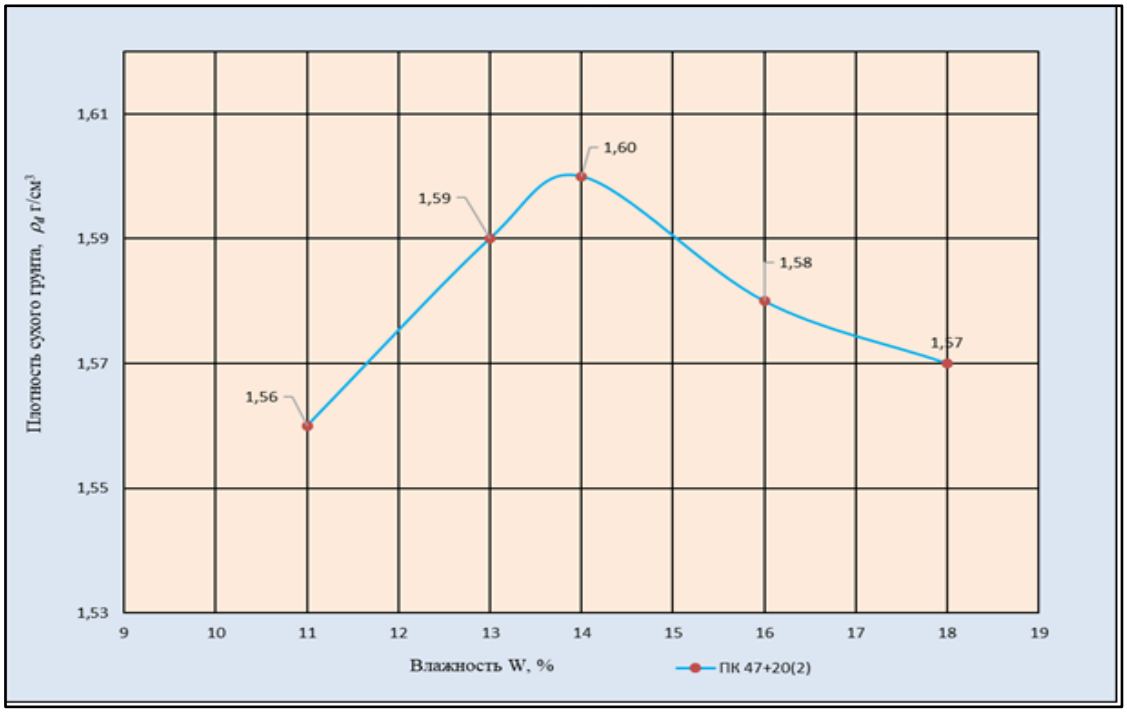

Figure 6. *Graph of the dependence of the maximum soil density on the optimal humidity. PK47+20(2). Standard A1.*

The average density of soil laid in a structure is assigned for structures up to 70 m high. equal to $0.95\rho_d^{max}$. and above 70 m. equal to $0.98\rho_d^{max}$. with a coefficient of variation V of no more than 0.05.

Humidity and density of soil during the construction of the Bustan canal at pickets where cracks appeared.

Table 5. *Results of laboratory soil testing*

PK	Canal side	Actual moisture content %	Dry density g/cm^3
47+20	left	19.2	1.54
		19.2	1.56
		19.8	1.51
202+80	left	17.9	1.68
		16.4	1.64
		20.5	1.56
		17.5	1.66
		16.0	1.66
		17.5	1.66
218.00	left	18.0	1.67
		17.9	1.68
		16.6	1.69
		16.4	1.65
		18.0	1.67

As can be seen from Table 5. during the construction of the embankment in areas where cracks appeared. the density ranges from 1.51 to 1.69 g/cm^3 at 16-20.5% of actual humidity.

4. Discussion and Conclusion

Researchers from many countries pay close attention to the appearance of cracks in concrete canals. This explains the relevance of the issue under consideration. The appearance of cracks reduces the efficiency of the canal. The reasons for the appearance of cracks are numerous depending on the climate. soil type. design errors. quality of construction work and others. We found that the soils in the samples from the place where the cracks appeared showed sandy loams and loams. and the borrow area soil was represented by sands. On PK47+20 (1) the soil is subsidence. which. together with other factors. may be the cause of the appearance of cracks.

Analyzing the data obtained. we can draw the following conclusions:

- According to their particle size distribution and plasticity number. samples belong to: PK 202+80 – sandy loam; PK 218+00 – sandy loam; PK47+20(1) - at the border of sandy loam and loam; PK47+20(2) - sandy loam. The borrow area soils in these areas are sandy.
- For three samples the relative subsidence strain is less than 0.01, i.e. the soil is non-subsidence. and for the first sample with PC 47+20 it changes from 0.014 to 0.019, i.e. subsidence soil. This may cause cracks at this location.
- According to Standard A1. the maximum density is ρ_{max} = 1.85 g/cm^3 with the humidity of the filling W_{opt} = 14%. while the density of the filling in the embankment body with a confidence probability of α = 0.95 will be ρ_d = 1.76 g/cm^3.
- According to standard A1. the maximum density is ρmax = 1.86 g/cm^3 with the humidity of the filling W_{opt} = 15%. while the density of the filling in the embankment body with a confidence probability of α = 0.95 will be ρ_d = 1.77 g/cm^3.
- According to Standard A1. the maximum density is ρmax = 1.78 g/cm^3 with the humidity of the filling W_{opt} = 15%. while the density of the filling in the embankment body with a confidence probability of α = 0.95 will be ρ_d = 1.69 g/cm^3.
- According to Standard A1. the maximum density is ρmax = 1.60 g/cm^3 with the humidity of the filling W_{opt} = 15%. while the density of the filling in the embankment body with a confidence probability of α = 0.95 will be ρ_d = 1.52 g/cm^3.
- During embankment construction. the density ranges from 1.51 to 1.69 g/cm^3 at 16-20.5% actual humidity.

5. References

Ahmadi, H., Rahimi, H., & Abdollahi, J. (2009). Optimizing the location of contraction–expansion joints in concrete canal lining. *Irrigation and Drainage*, 58(1), 116–125. Retrieved from https://doi.org/10.1002/ird.401

Bakhodir, K., Masharif, B., & Quvochbek, Y. (2023). Filtration reliability of the channel with concrete lining. *E3S Web of Conferences*, 410, 05024. Retrieved from https://doi.org/10.1051/e3sconf/202341005024

Belendir, N., Ivashintsov, A., & Stefanyshyn, D. (2004). *Methods for assessing the reliability of soil hydraulic structures. WRRI Publishing House named. B. E. Vedeneeva*.

GOST 22733-2002. (2002). *Soils. Laboratory method for determining maximum density*.

GOST 25100-2020. (2020). Soils. Classification.

GOST 28514-90. (1990). Determination of soil density using the volume replacement method.

He, P., Dong, J., Ren, X., & Wu, X. (2021). Longitudinal Deformation Model and Parameter Analysis of Canal Lining under Nonuniform Frost Heave. *Advances in Materials Science and Engineering*, 2021, 1–14. Retrieved from https://doi.org/10.1155/2021/5519035

Hu, J., Li, X., & Wang, C. (2023). Displacement prediction of deep excavated expansive soil slopes with high groundwater level based on VDM-LSSVM. *Bulletin of Engineering Geology and the Environment*, 82(8), 320. Retrieved from https://doi.org/10.1007/s10064-023-03329-7

Iskandar, P., Dinar Dwi Anugerah, P., & Putri Kusuma, W. (2021). Net present value (NPV) of the rehabilitated irrigation channels to increase agricultural production. *International Journal of Advanced Technology and Engineering Exploration*, 8(78), 576–583. Retrieved from https://doi.org/10.19101/IJATEE.2021.874034

Kosichenko, Yu. M. (2006). Investigation of seepage losses from canals of irrigation systems. *Land Reclamation and Water Management.*, 6, 24–26.

Kosichenko, Yu. M., Bae, O. A., & Ishchenko, A. V. (2014). Modern methods of against filtration in irrigation systems. *Engineering Bulletin of the Don*, 3, 13.

Kosichenko, Yu. M., & Baev, O. (2020). Efficiency and durability of the linings channels of geosynthetics. *Magazine of Civil Engineering*. Retrieved from https://doi.org/10.18720/MCE.96.4

Kulumbetov B.P., Bakiev M.R., K. Kh. Kh. (2023). Construction of a canal embankment from sandy soils. (in Russian). *Irrigatsiya va Melioratsiya*, 4(24), 23–28.

Liu, H., Ma, D., Wang, C., Liu, X., Wu, D., & Khan, K. U. J. (2021). Study on the frost heave mechanism of the water conveyance canal and optimized design of slope protection. *Bulletin of Engineering Geology and the Environment*, 80(11), 8397–8417. Retrieved from https://doi.org/10.1007/s10064-021-02447-4

Lunyov A.A. (2019). *Justification of the calculated values of the mechanical values of the mechanical characteristics of ash and slag mixtures for the design of roadbed (in Russian)*.

Rahimi, H., & Barootkoob, SH. (2002). Concrete canal lining cracking in low to medium plastic soils. *Irrigation and Drainage*, 51(2), 141–153. Retrieved from https://doi.org/10.1002/ird.41

Rahimi, Hassan, & Abbasi, N. (2008). Failure of concrete canal lining on fine sandy soils: a case study for the Saveh Project. *Irrigation and Drainage*, 57(1), 83–92. Retrieved from https://doi.org/10.1002/ird.350

Rahimi, Hassan, Abbasi, N., & Shantia, H. (2011). APPLICATION OF GEOMEMBRANE TO CONTROL PIPING OF SANDY SOIL UNDER CONCRETE CANAL LINING (CASE STUDY: MOGHAN IRRIGATION PROJECT, IRAN). *Irrigation and Drainage*, 60(3), 330–337. Retrieved from https://doi.org/10.1002/ird.574

Taran, F., & Mahtabi, G. (2020). Optimum layout of weep holes in concrete irrigation canals to control uplift pressure and hydraulic gradient. *Arabian Journal of Geosciences*, 13(2), 88. Retrieved from https://doi.org/10.1007/s12517-020-5108-3

Wang, Z., Zhang, M., Li, G., & Liu, W. (2023). A mechanical model for trapezoidal canals lined with geomembranes and anti-slip material during freezing-thawing processes. *Cold Regions Science and Technology*, 208, 103783. Retrieved from https://doi.org/10.1016/j.coldregions.2023.103783

Yao, L., Feng, S., Mao, X., Huo, Z., Kang, S., & Barry, D. A. (2012). Coupled effects of canal lining and multi-layered soil structure on canal seepage and soil water dynamics. *Journal of Hydrology*, 430–431, 91–102. Retrieved from https://doi.org/10.1016/j.jhydrol.2012.02.004

Zhu, R., Huang, Y., Zhang, C., Guo, W., & Chen, H. (2022). Laboratory and centrifugal model tests on failure mechanism of canal slopes under cyclic action of wetting–drying. *European Journal of Environmental and Civil Engineering*, 26(7), 2819–2833. Retrieved from https://doi.org/10.1080/19648189.2020.1773321